

[Journal Name]

Supporting Information for

Deep structure of the Grenada Basin from wide-angle seismic, bathymetric and gravity data

Crelia Padron^{1,2}, Frauke Klingelhoefer², Boris Marcaillou³, Jean-Frédéric Lebrun⁴, Serge Lallemand⁵, Clément Garrocq⁵, Mireille Laigle³, Walter R Roest², Marie-Odile Beslier³, Laure Schenini³, David Graindorge⁶, Aurelien Gay⁵, Franck Audemard⁷, Philippe Münch⁵ and the GARANTI cruise team

1 Departamento de Ciencias de la Tierra, Universidad Simón Bolívar (USB), Caracas, Venezuela.

2 Géosciences Marines, Ifremer, ZI de la Pointe du Diable, CS 10070, 29280 Plouzané France

3 Geoazur, Université Côte d'Azur, CNRS, IRD, Observatoire de la Côte d'Azur, Géoazur, 250 Avenue Albert Einstein, 06560 Valbonne, France

4 Géosciences Montpellier, Université des Antilles, CNRS, Université de Montpellier, Campus de Fouillole, Pointe-à-Pitre, Guadeloupe (FWI)

5 Géosciences Montpellier, CNRS, Université de Montpellier, Université des Antilles, Place Eugène Bataillon, 34095 Montpellier, France

6 Laboratoire Géosciences Océan, CNRS-UBO-UBS, Université Bretagne Pays de Loire (UBL), Brest, Institut Universitaire Européen de la Mer, rue Dumont Durville, F-29280, Plouzané, France.

7 Venezuelan Foundation for Seismological Research, El Llanito, Caracas, Venezuela.

Contents of this file

Text S1 to S2
Figures S1 to S10

Introduction

This electronic supplements file presents some of the data figures of the main manuscript in a larger scale for better visibility, as well as additional text and figures regarding the model quality. A figure showing the position of wide-angle seismic profiles compared to our study has also been included.

Text S1.

The data quality was very good with usable arrivals to offsets over 100 km on some data sections. Record sections from the basin allowed to differentiate the sedimentary layers and the Moho depth was reached along all three profiles. Travel-time picking was undertaken on time reduced sections. Where possible, sections without frequency filters applied were used, but at long offsets or in sections with a high noise level, picking was done along bandpass filtered sections. Most turning wave arrivals were picked along the vertical geophone channel, however reflected arrivals were often better imaged in the hydrophone section. Comparison between the reflections in the unreduced OBS-sections shifted to simulate two-way travel-times and reflection seismic sections helped to define the different layers in the sedimentary cover. The modeling was done with a forward approach and the inversion tool of the *Rayinvr* software was mainly used for fine-tuning the model. Amplitude modeling was used to better constrain the velocities gradients in the different layers.

Text S2.

The ray hit count is a measure of the number of rays passing through a particular area. It provides a measure of how well a section of the subsurface is sampled by the seismic survey and could be thus well resolved (see Figures S1, S2, S3), providing crossing rays with varying incidence angles. Although regions of low ray hit-count values are less well constrained, care was taken during modeling to use the minimum structure approach (Zelt, 1999) to avoid over-interpretation. Hit count values are high (> 5000) in the sedimentary layer and lower in the crustal layers. If a model parameter is poorly resolved a given perturbation will be smeared into adjacent regions. So, the smearing factor gives information about the influence of perturbations of one single node onto the neighboring velocity and depth nodes (see Figures S1, S2, S3 and detailed explanation in Zelt, 1999).

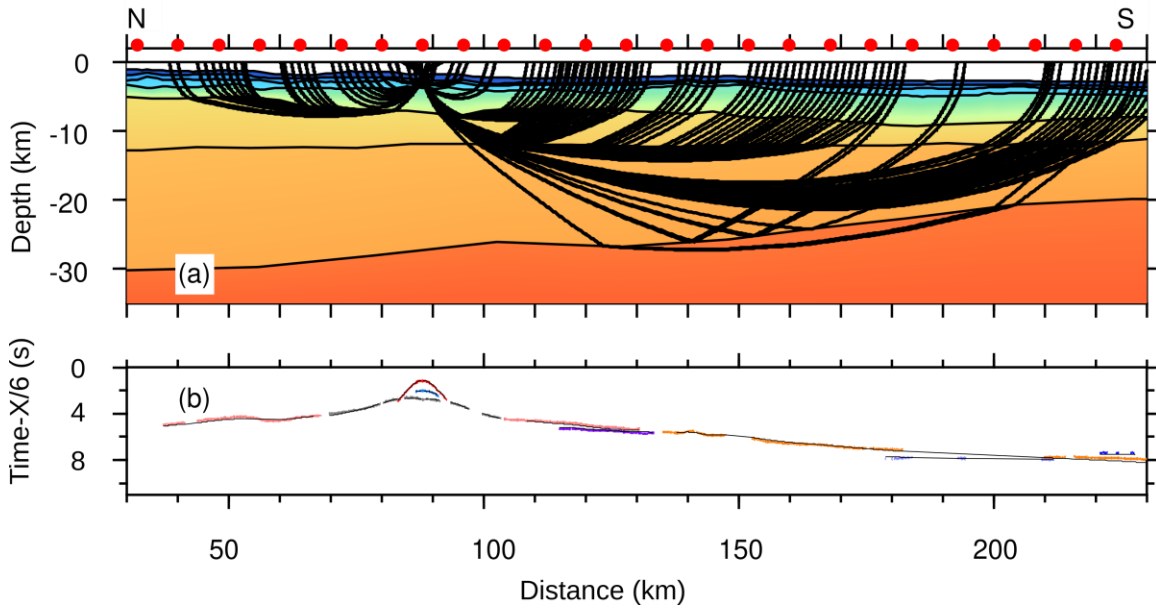


Figure S1. (a) Model layers and ray-paths of every 10th ray (b) corresponding to travel-time picks and predicted arrivals (black lines) OBSs 1-12 on profile GA01 OBS positions are marked by red dots on top of each profile's model layers. Color scale is identical to Figure 6 in the main text.

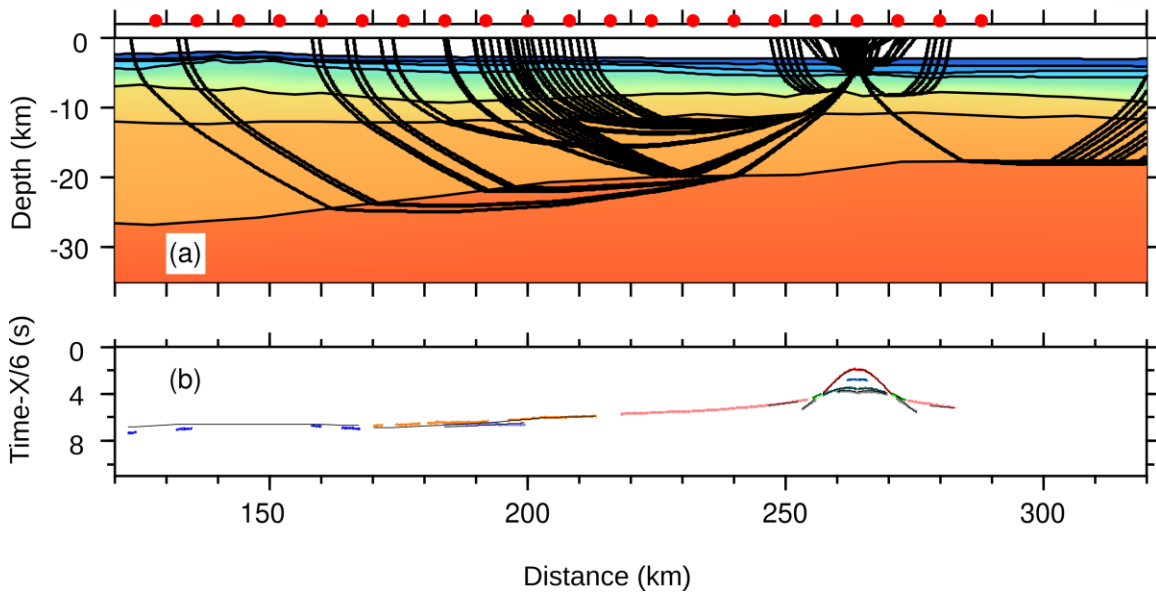


Figure S2. (a) Model layers and ray-paths of every 10th ray (b) corresponding to travel-time picks and predicted arrivals (black lines) OBSs 1-34 on profile GA01 OBS positions are marked by red dots on top of each profile's model layers. Color scale is identical to Figure 6 in the main text.

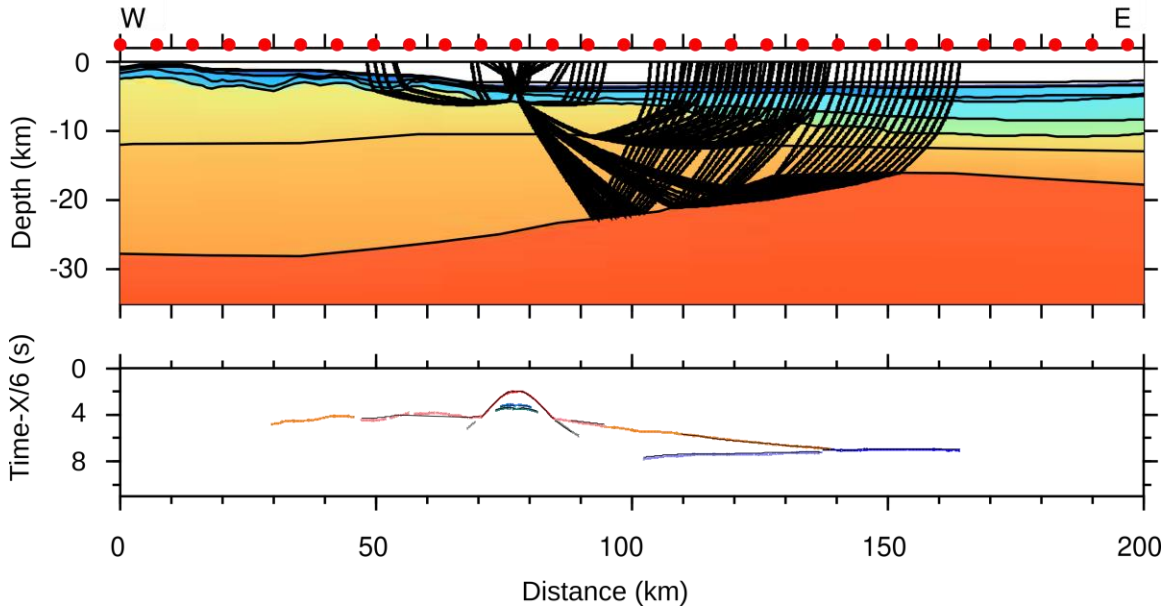


Figure S3. (a) Model layers and ray-paths of every 10th ray (b) corresponding to travel-time picks and predicted arrivals (black lines) OBSs 2-12 on profile GA02 OBS positions are marked by red dots on top of each profile's model layers. Color scale is identical to Figure 6 in the main text.

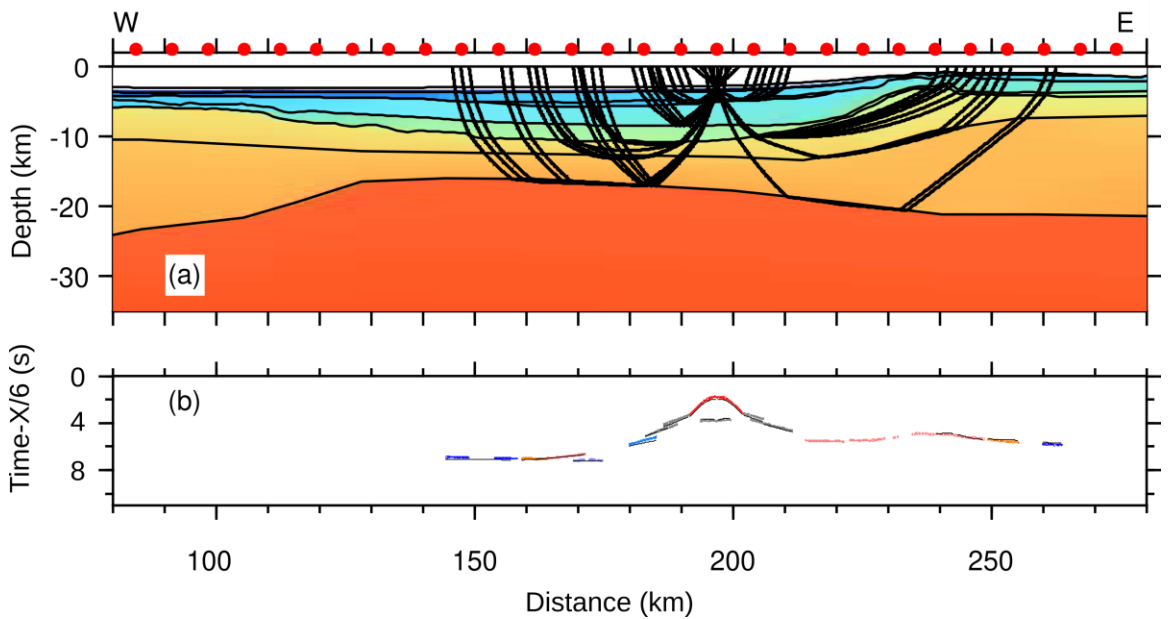


Figure S4. (a) Model layers and ray-paths of every 10th ray (b) corresponding to travel-time picks and predicted arrivals (black lines) OBSs 2-29 on profile GA02 OBS positions are marked by red dots on top of each profile's model layers. Color scale is identical to Figure 6 in the main text.

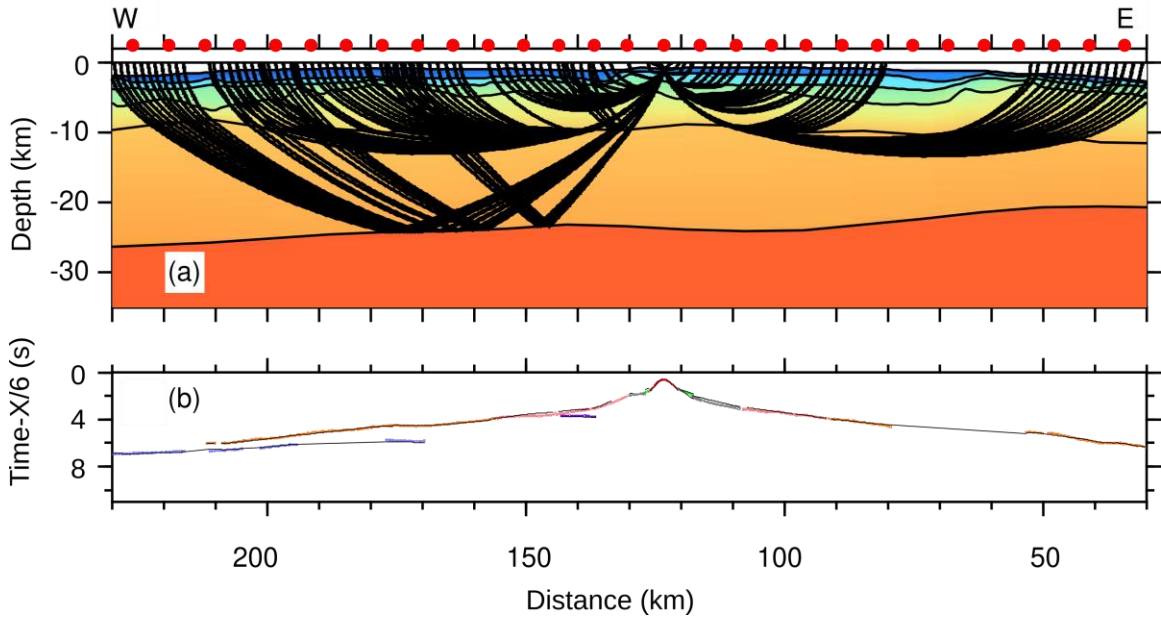


Figure S5. (a) Model layers and ray-paths of every 10th ray (b) corresponding to travel-time picks and predicted arrivals (black lines) OBSs 3-19 on profile GA03 OBS positions are marked by red dots on top of each profile's model layers. Color scale is identical to Figure 6 in the main text.

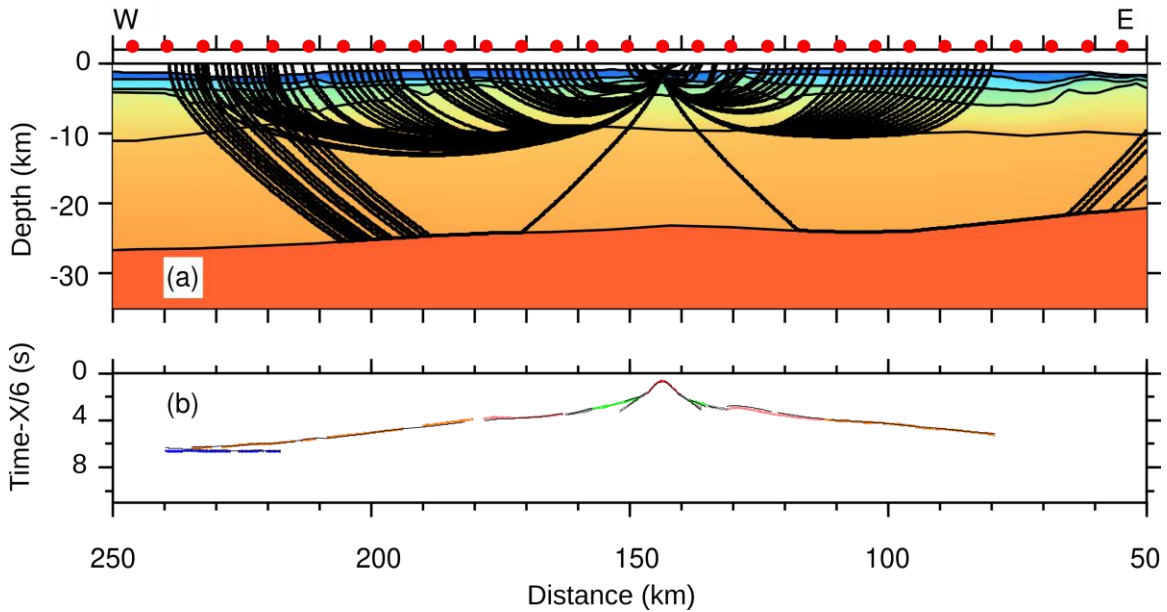


Figure S6. (a) Model layers and ray-paths of every 10th ray (b) corresponding to travel-time picks and predicted arrivals (black lines) OBSs 3-22 on profile GA03 OBS positions are marked by red dots on top of each profile's model layers. Color scale is identical to Figure 6 in the main text.

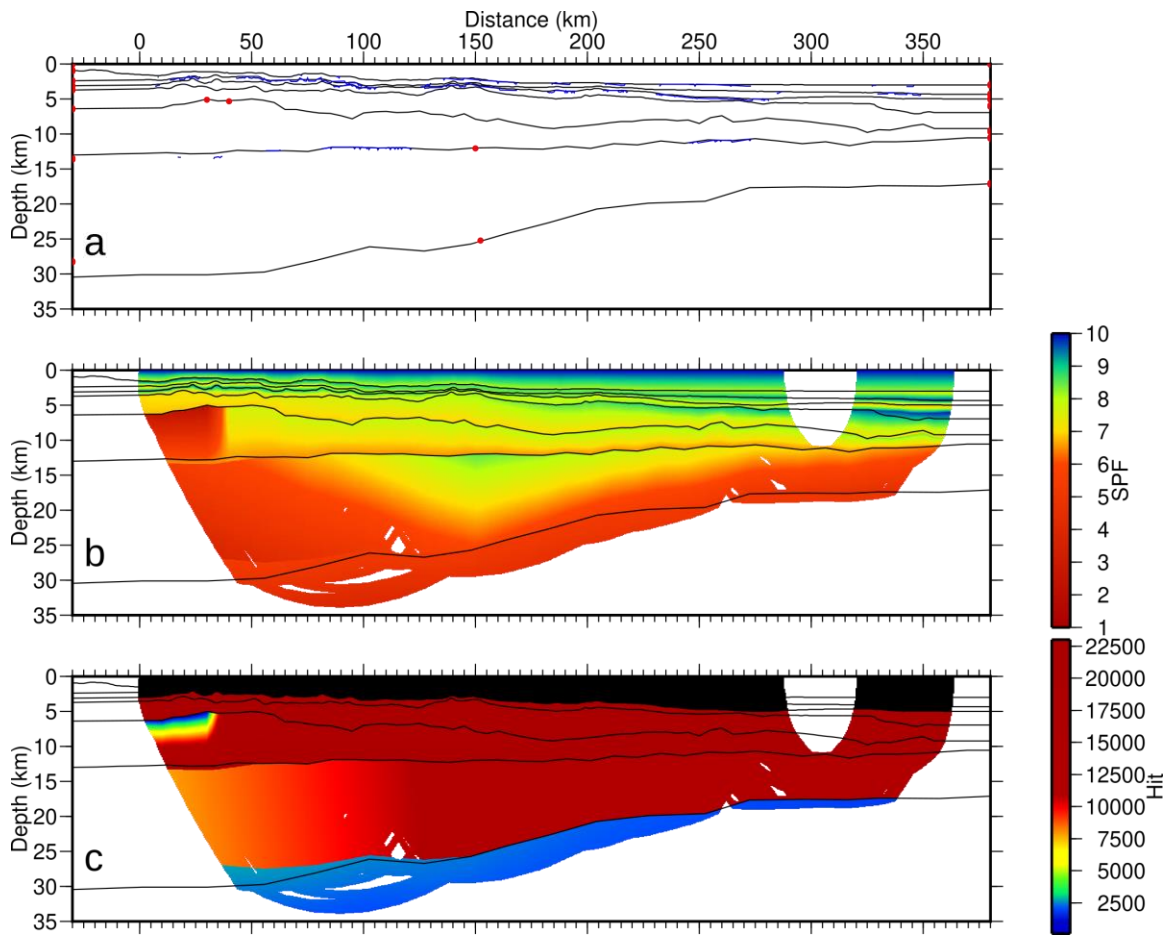


Figure S7. Error estimation of the GA01 velocity model. (a) Model parameterization including interface depth, top and bottom layer velocity nodes (red circles). (b) Spread-Point function (SPF) for velocity (gridded and colored) nodes. (c) Hit count for velocity (gridded and colored) nodes.

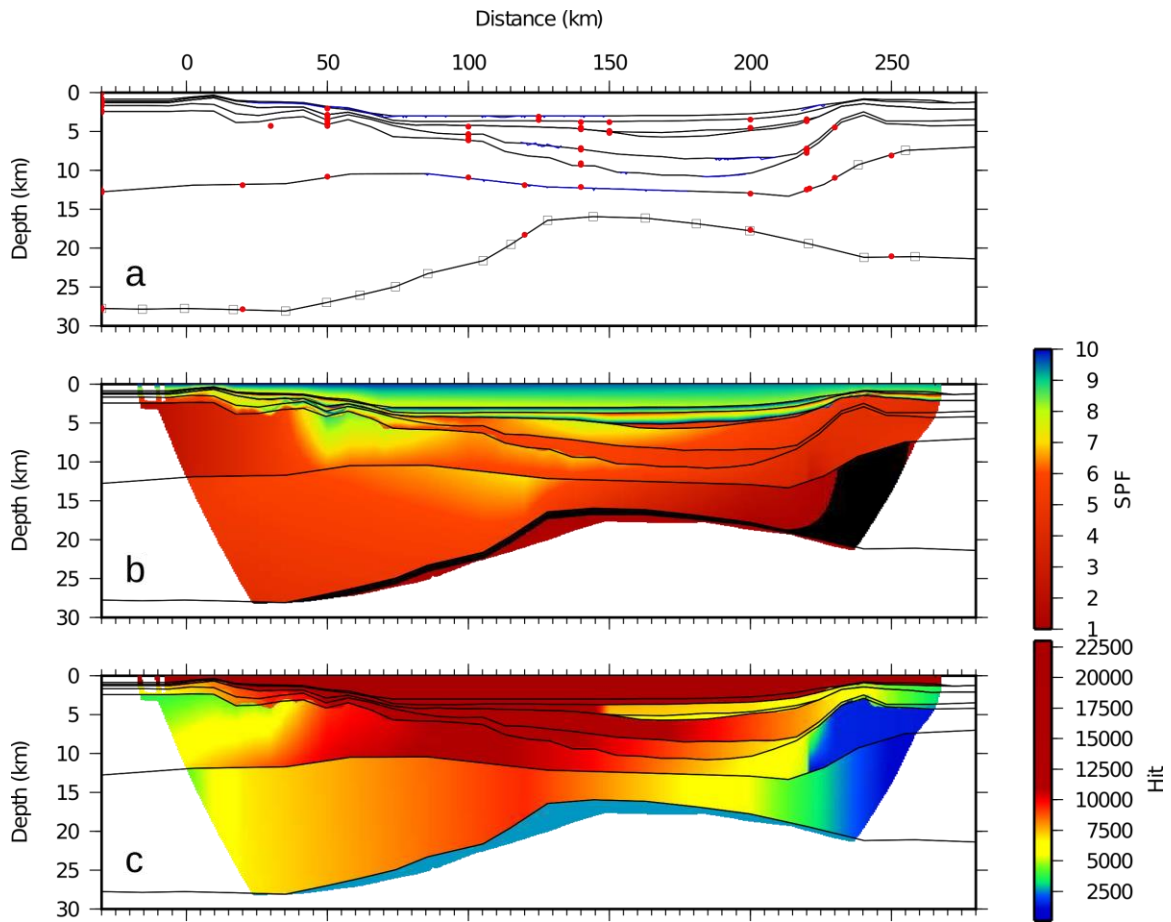


Figure S8. Error estimation of the GA02 velocity model. (a) Model parameterization including interface depth, top and bottom layer velocity nodes (red circles). (b) Spread-Point function (SPF) for velocity (gridded and colored) nodes. (c) Hit count for velocity (gridded and colored) nodes.

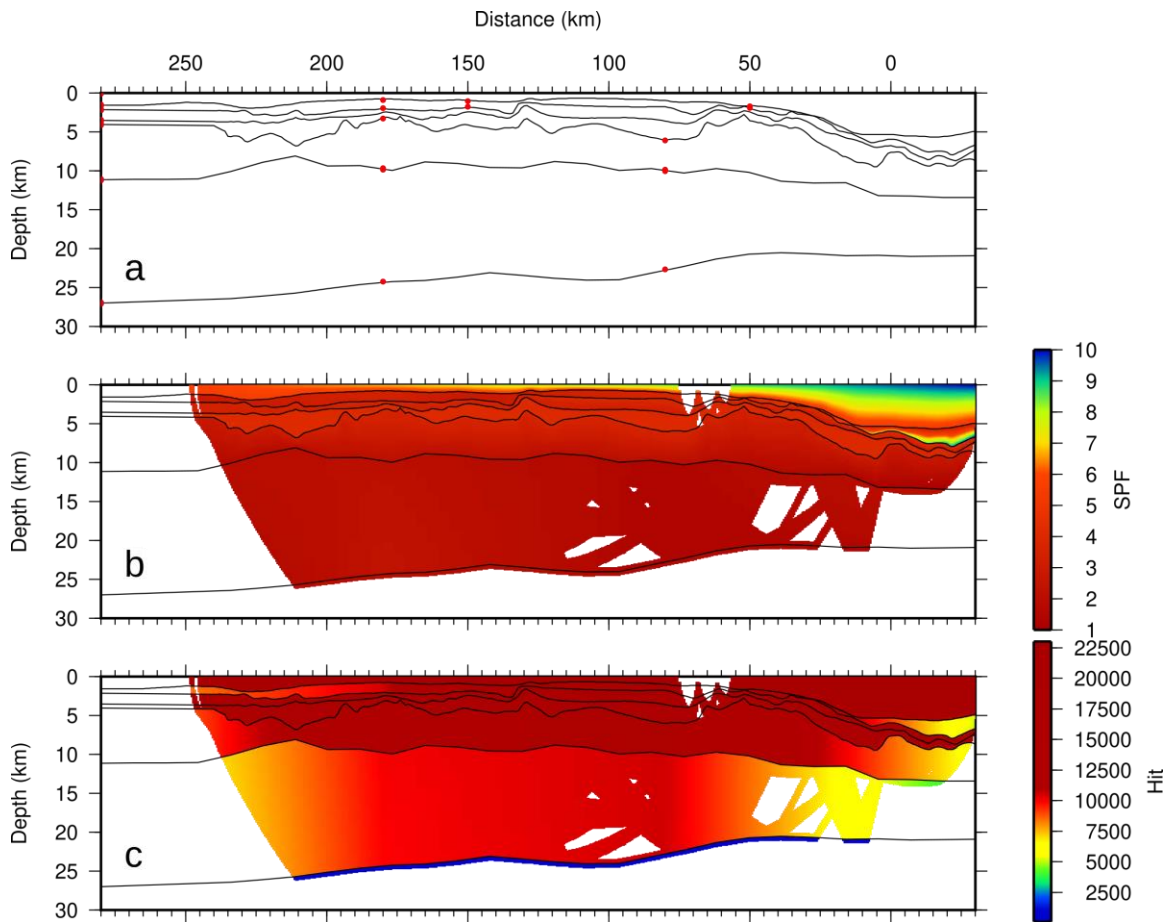


Figure S9. Error estimation of the GA03 velocity model. (a) Model parameterization including interface depth, top and bottom layer velocity nodes (red circles). (b) Spread-Point function (SPF) for velocity (gridded and colored) nodes. (c) Hit count for velocity (gridded and colored) nodes.

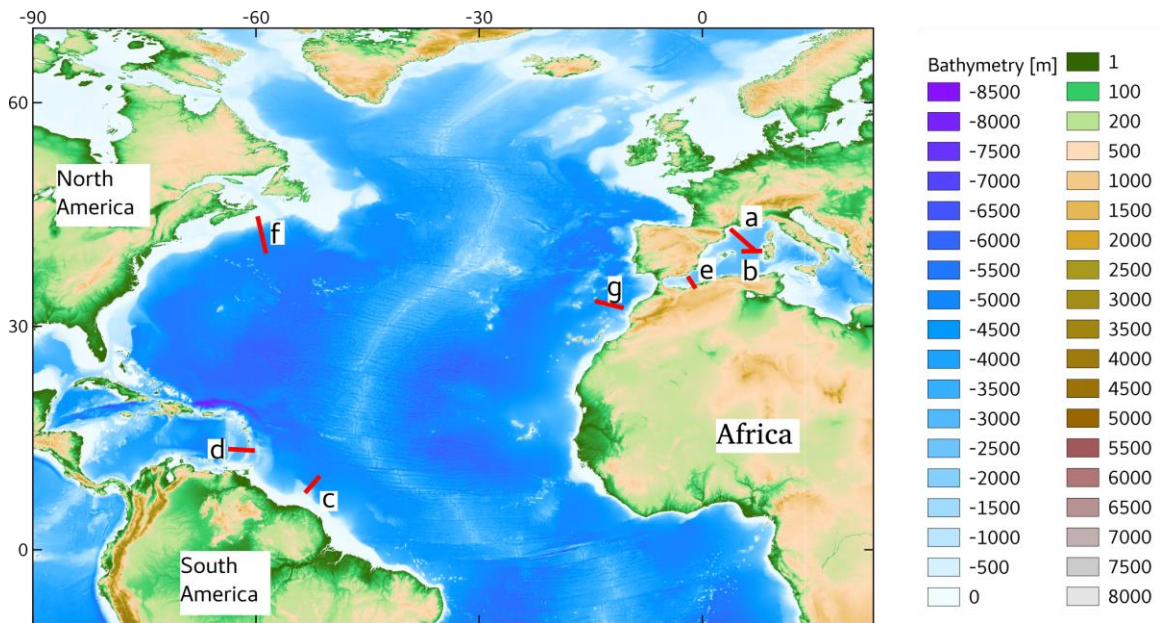


Figure S10. Location map showing the position of the comparison profiles from main text Figure 18.